A&A 546, A48 (2012)
DOI: 10.1051/0004-6361/201219916

Astronomy & Astrophysics

The star formation histories of Hickson compact group galaxies

I. Plauchu-Frayn[1], A. Del Olmo[1], R. Coziol[2], and J. P. Torres-Papaqui[2]

[1] Instituto de Astrofísica de Andalucía IAA – CSIC, Glorieta de la Astronomía s/n, 18008 Granada, Spain
e-mail: ilse@iaa.es
[2] Departamento de Astronomía, Universidad de Guanajuato, Apdo. Postal 144, 36000 Guanajuato, Gto., Mexico

Received 28 June 2012 / Accepted 8 August 2012

ABSTRACT

Aims. We study the star formation fistory (SFH) of 210 galaxy members of 55 Hickson compact groups (HCG) and 309 galaxies from the Catalog of Isolated Galaxies (CIG). The SFH traces the variation of star formation over the lifetime of a galaxy, and consequently yields a snapshot picture of its formation. Comparing the SFHs in these extremes in galaxy density allows us to determine the main effects of compact groups (CG) on the formation of galaxies.

Methods. We fit our spectra using the spectral synthesis code STARLIGHT and obtained the stellar population contents and mean stellar ages of HCG and CIG galaxies in three different morphological classes: early-type galaxies (EtG), early-type spirals (EtS), and late-type spirals (LtS).

Results. We find that EtG and EtS galaxies in HCG show higher contents of old and intermediate stellar populations as well as an important deficit of the young stellar population, which clearly implies an older average stellar age in early galaxies in HCG. For LtS galaxies we find similar mean values for the stellar content and age in the two samples. However, we note that LtS can be split into two subclasses, namely old and young LtS. In HCG we find a higher fraction of young LtS than in the CIG sample, in addition, most of these galaxies belong to groups in which most of the galaxies are also young and actively forming stars. The specific star formation rate (SSFR) of spiral galaxies in the two samples differ. The EtS in HCG show lower SSFR values, while LtS peak at higher values compared with their counterparts in isolation. We also measured the shorter star formation time scale (SFTS) in HCG galaxies, which indicates that they have a shorter star formation activity than CIG galaxies. We take these observations as evidence that galaxies in CG have evolved more rapidly than galaxies in isolation, regardless of their morphology. Our observations are consistent with the hierarchical galaxy formation model, which states that CGs are structures that formed recently from primordial small-mass density fluctuations. From the systematic difference in SFTS we deduce that the HCG have most probably formed ~3 Gyr in the past. The galaxies in the HCG are not in equilibrium state, but merging without gas (i.e., under dissipationless conditions), which may explain their relatively long lifetime.

Key words. galaxies: evolution – galaxies: groups: general – galaxies: interactions – galaxies: stellar content

1. Introduction

Compact groups (CG) of galaxies are local structures with high galaxy densities, equivalent to what is measured in the centers of galaxy clusters. In constrast to clusters, however, the velocity dispersion of the galaxies in CG is low, comparable to the velocity dispersion of elliptical galaxies or the rotational velocity of spiral disks (Hickson 1997, and references therein). These conditions favor interactions, and even mergers, which suggests that galaxies in CG must show much evidence of these phenomena, either happening now, or having happened in the past. However, after almost forty years of studies, it still remains an open question how CG really formed.

One of the most extensively studied samples of CG is the Hickson compact group (HCG) catalog as defined by Hickson (1982). Subsequent spectroscopy studies have shown that the majority of the HCG have galaxies with concordant redshifts (Hickson et al. 1992), which display many signs of interactions in the form of tidal tails, tidal bridges, distorted isophotes, faint shells, and double nuclei (Mendes de Oliveira & Hickson 1994; Hickson 1997; Vílchez & Iglesias-Páramo 1998; Verdes-Montenegro et al. 2001, 2002, 2005; Coziol & Plauchu-Frayn 2007; Plauchu-Frayn & Coziol 2010a). Asymmetrical rotation curves have also been detected (Rubin et al. 1991; Nishiura et al. 2000; Torres-Flores et al. 2010) and, contrary to what was assumed in the past, various evidence for present and past mergers has also clearly been established (Caon et al. 1994; Coziol & Plauchu-Frayn 2007; Plauchu-Frayn & Coziol 2010b). All these observations are consistent with the initial assumption which, sustains that CG are physically real structures in which galaxies have experienced frequent dynamical interactions during their formation and evolution.

Other aspects of CG, on the other hand, still defy our comprehension. Spectroscopy study results, in particular, were found to be different from expectations based on the common assumptions that the main effects of dynamical interactions on galaxies in CG should be a direct enhancement of their star formation and activation of supermassive black holes (SMBHs) at their centers. Although emission-line galaxies are remarkably frequent in CG, involving more than 50% of the galaxies (Coziol et al. 1998, 2000, 2004; Martínez et al. 2008, 2010), this activity seems mostly nonthermal, in the form of Seyfert 2, low-ionization nuclear emission-line region (LINER), and numerous low-luminosity active galactic nuclei (AGN). Luminous AGN with typical broad line regions are relatively rare in CG (Coziol et al. 1998, 2004; Ribeiro et al. 1996; Martínez et al. 2008, 2010). Nuclear star formation, although mildly enhanced in some groups (e.g., Ribeiro et al. 1996; Iglesias-Páramo & Vílchez 1997), is generally low (Rubin et al. 1991; Zepf et al. 1991; Moles et al. 1994;

Pildis et al. 1995; Menon 1995; Ribeiro et al. 1996; Coziol et al. 1998, 2000; Verdes-Montenegro et al. 1998; Allam et al. 1999; Iglesias-Páramo & Vílchez 1999; Martínez et al. 2010).

In part, the observation that star formation is possibly deficient and that AGN are mostly underluminous in CG could be due to a general deficiency of gas. One possibility is that this is the effect of tidal gas stripping. However, although evidence of tidal gas stripping is unquestionable in CG (e.g., Verdes-Montenegro et al. 2001; Durbala et al. 2008), this mechanism alone cannot explain all observations. In particular, tidal gas stripping cannot explain the higher fraction of early-type galaxies found in CG (Hickson 1982; Williams & Rood 1987; Sulentic 1987; Hickson et al. 1988; Palumbo et al. 1995). Indeed, it is difficult to explain how an elliptical galaxy, or even the massive bulge of an early-type spiral galaxy, can build up after star formation is quenched in the disk of a late-type spiral galaxy by gas stripping (Dressler 1980), unless one assumes that these galaxies can build massive bulges later by dry mergers (Plauchu-Frayn & Coziol 2010b). However, neither can gas stripping explain the many AGN observed in CG (e.g., Coziol et al. 1998, 2000; Martínez et al. 2010). These AGN are related to the formation of numerous early-type galaxies through tidal triggering, a mechanism that funnels gas down directly into the center of galaxies, starting a sequence of bursts of star formation that increase the mass of the bulges, and forming, or feeding, a SMBH at their centers (Merritt 1983, 1984; Byrd & Valtonen 1990; Henriksen & Byrd 1996; Fujita 1998). However, because the level of these activities is generally low, we would then have to assume that these events have taken place sometime in the recent past, or possibly during the formation of the CG (Coziol et al. 2004; Mendes de Oliveira et al. 2005). The important question is, how long ago?

Recent studies using Lick indices to determine the stellar population contents of elliptical galaxies in small samples of HCG have shown that the formation process of these galaxies is similar to that of ellipticals in clusters of galaxies (Proctor et al. 2004; Mendes de Oliveira et al. 2005; de la Rosa et al. 2007), and suggested that their formation took place at least 2 Gyr in the past. This is already older than predicted by the fast merger scenario for CG, which has led some authors (e.g., Proctor et al. 2004; Mendes de Oliveira et al. 2005) to propose that CG are defying the standard cosmological model of structure formation. However, this conclusion is somewhat premature, considering our current state of comprehension of the physics behind all the processes involved this model.

Many aspects of CG as described above would instead seem to be in reasonably good agreement with the basic predictions of the standard model of structure formation. Coziol et al. (2009) suggested that CG are the building blocks of larger-scale structures such as clusters of galaxies. Consistent with the hierarchical galaxy formation model (White & Frenk 1991; Kauffmann et al. 1993; Cole et al. 1994), galaxies form from primordial fluctuations in mass density. In regions showing higher fluctuations, the galaxy formation process starts earlier than in regions with lower fluctuations. Assuming the power law for the mass function of the fluctuations is relatively steep, the first structures that form would look like massive CG, where the low-velocity dispersions of the protogalaxies in these systems favor interactions and mergers that produce numerous massive elliptical and early-type spiral galaxies through a sequence of starbursts. The increased potential wells of these newly assembled structures would then attract other similar systems, and much primordial gas would eventually fall in, being enriched in the process by the metals expelled from galaxies by starburst winds (Torres-Papaqui et al. 2012). Much later, late-type spirals that formed in isolation in the field would eventually fall in, making the final structure consistent with a cluster of galaxies. According to the hierarchical galaxy formation model, in low-mass density fluctuations the same process would be expected to start later, resulting in slightly different results because of the small amounts of mass available.

Within the above theoretical context, our present knowledge of CG may suggest two different formation scenarios. According to the first scenario, galaxies in CG have formed first in relative isolation, first from very low-mass density fluctuations consistent with the field, which more likely formed a gas-rich disk, then later on (i.e. at the present epoch) started to form a more gravitationally bound structure like the CG. Within this scenario, tidal gas stripping, quenching star formation in disk galaxies, and dry mergers, which would grow more massive bulges, would play the central role in the evolution of CG. The second scenario is more similar to what may have happened during the formation of clusters. Galaxies forming the CG never assumed a spiral form before, but merged rapidly as gas-rich protogalaxy systems. Through multiple interactions, triggering starbursts and gas funneling, galaxies form massive bulges, many with an active black hole at their center. However, considering the low density of the matter in which these galaxies formed, and a first phase of intense star formation and AGN activity, short timescales for gas consumption would ensue. Reaching a pure elliptical structure in these conditions would not always be possible, and the expected end products would instead be several gravitationally bounded, relatively gas-deficient, early-type spiral galaxies, with an aging SMBH at their center that accretes at lower rates than in the field (consistent with a low luminosity AGN). As in the model for the formation of clusters, during the first phase of the CG formation a deeper gravitational potential well builds up, which then acts as a pole of attraction for late-type galaxies that formed at the periphery, making the final structures similar to CG.

To distinguish between these scenarios for the formation of CG we used the stellar population synthesis code STARLIGHT[1] (Cid Fernandes et al. 2005) to determine the star formation histories (SFHs) of 210 galaxies members in 55 HCGs. The SFH traces the variation of star formation over the lifetime of a galaxy, and consequently yields a snapshot picture of its formation. For comparison we also determined the SFHs of 309 galaxies taken from the Catalog of Isolated Galaxies (CIG), which represent the lowest galaxy density regime. Our study is organized in the following manner. In Sect. 2 we describe the selection of our two different samples. In Sect. 3 we explain the spectra synthesis method. In Sect. 4 we present the results of our comparison of the SFHs in our different samples. In Sect. 5 we briefly discuss the consequence of these results and expose our main conclusions. Throughout this study a Hubble constant $H_0 = 75\ \mathrm{km\,s^{-1}\,Mpc^{-1}}$ is assumed.

2. Selection of the samples and observational data

2.1. Compact group galaxies

To determine our sample of galaxies in CG, we started with the sample of 64 HCGs (Hickson 1982), which was used by Martínez et al. (2010, hereafter M10) to determine the nature of the nuclear activity of the galaxies in these systems. These data comprise medium-resolution long-slit spectroscopy in the

[1] http://www.starlight.ufsc.br

optical range 3600–7200 Å. They were obtained using four telescopes: the 2.2 m telescope in Calar-Alto (CAHA, Spain), the 2.56 m NOT Telescope at the Observatorio del Roque de los Muchachos (ORM) in La Palma (Spain), the 2.12 m telescope at the Observatorio Astronómico Nacional in San Pedro Mártir (SPM) in Baja California (México), and the 1.5 m telescope operated by the IAA in the Sierra Nevada Observatory (OSN, Spain). The observations were performed using a reciprocal dispersion of 2 Å/px at CAHA and OSN, 3 Å/px at the NOT ALFOSC spectrograph and 4.3 Å/px in SPM. A detailed description of the instrumental setups, the log of observations, and reduction procedures were presented in M10 (Tables 2 and 3) and in Martínez et al. (2008). Also included in those references are the characteristics of the final one-dimensional nuclear spectra such as the extracted apertures for each galaxy, which in general correspond to the central 1 kpc region.

The total number of galaxies in the 64 HCG amounts to 269, while in M10 we found the spectra of only 220 of these galaxies (82% of the sample). In an effort to complete our sample, we searched the Sloan Digital Sky Survey Data Release 7 (SDSS-DR7; Abazajian et al. 2009) and found the spectra for 68 galaxies. However, 63 of these galaxies were already in the M10 sample. Comparing the signal-to-noise ratio, S/N, around three different λ windows (centered at $\lambda = 4750$ Å, $\lambda = 5525$ Å, and $\lambda = 6825$ Å), we kept 57 spectra from SDSS and 6 of M10, applying the criterion that $S/N \geq 5$. We also discarded 15 galaxies from M10 because they were observed only in the red or because they did not pass our S/N criterion. Our final complete sample consists, therefore, of 210 galaxies in 55 HCG (148 galaxies from M10 and 62 from SDSS). All these galaxies have concordant redshift (Hickson et al. 1992), up to $z = 0.045$, and are members of groups with a surface brightness $\mu_g \geq 24$ mag arcsec^2. All morphologies for the galaxies in our sample were extracted from the online compilation HYPERCAT[2] (Paturel et al. 1994, 1997).

2.2. Isolated galaxies

To build our sample of isolated galaxies, we used the Catalog of Isolated Galaxies (CIG; Karachentseva 1973). In this catalog, a galaxy with a standard angular diameter D is classified as isolated when all its neighbors, with angular diameters d, are located at a projected distance not closer than $20d$. Physically, this criterion should imply that a galaxy has not suffered any gravitational influence from nearby galaxies over the last billion years. In absence of external influence, the evolution of these galaxies is consequently assumed to be driven mainly by internal processes.

In their study of isolated galaxies, Verley et al. (2007) refined the isolation criterion by taking into account not only the local number density of neighbor galaxies, a parameter they identified as η_k, but also the tidal strength per unit mass, Q, that is produced by all the neighbors. By applying these criteria, these authors have reduced the number of galaxies in the CIG by 16%, producing a list of 791 "most isolated" galaxies (defined to have $\eta_k \leq 2.4$, and $Q \leq -2$). Starting with this list and applying our S/N criterion, we extracted from SDSS the spectra of 309 of these galaxies, which form our final sample of CIG. The morphologies for these galaxies were extracted from Sulentic et al. (2006) and HYPERCAT.

[2] http://www-obs.univ-lyon1.fr/hypercat

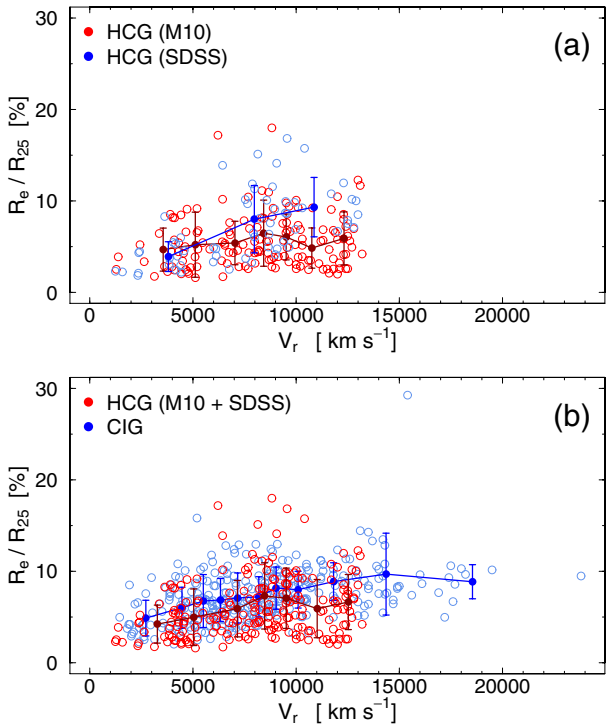

Fig. 1. Equivalent radius-to-25 mag arcsec^{-2} isophote radius ratio as a function of the radial velocity of galaxies. **a)** Comparison between spectra taken from Martínez et al. (2010) and SDSS for the HCG sample and **b)** comparison between the HCG and CIG samples. In each panel, the lines join the mean values determined in sets of **a)** 20 and **b)** 30 galaxies at different redshifts. The error bars give the standard deviation of the means.

2.3. Quantifying aperture biases

Because the spectra come from two different databases and have been taken with different instruments, we verified that they are comparable and suitable for our study. The spectral resolution of the spectra, which are both in the medium range, is not a problem. Both have the value required to be adjustable to the stellar library resolution used by STARLIGHT. On the other hand, the SDSS spectra have been taken with a fixed fiber circular aperture, while the M10 spectra have been taken with a long-slit aperture.

For compatibility's sake, we checked to see if the extracted spectra cover similar physical spatial areas. To do so, we calculated the equivalent radius, R_e, covered by the long-slit and fiber apertures and compared these values with the radius R_{25}, which corresponds in a galaxy to the radius of the 25 mag arcsec^{-2} isophote. In Fig. 1 we compare the percentage of R_{25} covered by R_e in our samples. In our HCG sample, the mean value of R_e/R_{25} is (5 ± 3)% and (7 ± 4)% for spectra taken from M10 and SDSS, respectively, while in the CIG sample this is (7 ± 3)%. In Fig. 1a we plot R_e/R_{25} for galaxies in M10 and SDSS for HCG sample and in Fig. 1b the same comparison is shown between the HCG and CIG samples. In this figure, the continuous lines join the mean values determined in sets of 20 and 30 galaxies taken at different redshifts (Fig. 1a and b, respectively), and the error bars give the standard deviations of the means. The means are comparable to the medians in both samples, and no systematic difference is observed in R_e/R_{25} for spectra obtained from different databases, instruments and samples. A few isolated galaxies are found at higher redshift, but with no significant increase in the ratio R_e/R_{25}. In general, the similar low means imply that

Table 1. Morphological class distributions in the samples.

Morphological class	Types	HCG	CIG
No. of gal.		210	309
early-type galaxies (EtG)	E-S0	38%	16%
early-spirals (EtS)	S0a-Sb	37%	28%
late-spirals (LtS)	Sbc and later	25%	56%

in both samples the light from the spectra comes from comparable regions in the most central part of the galaxies (∼1–2 kpc^2). Therefore, we conclude that there is practically no difference in aperture between the spectra that could influence our results.

2.4. Morphology distributions

It is well known that galaxies in the nearby universe follow a morphology-density relation (Dressler 1980; Whitmore et al. 1993; Deng et al. 2008), according to which early-type galaxies are more clustered than late-type galaxies. The HCG are no exception, the fraction of galaxies with early-type morphologies being generally higher than in the field (Hickson 1982; Williams & Rood 1987; Hickson et al. 1988). Therefore, a statistical comparison of SFH between extreme-density regimes needs to account for differences in morphological distribution. For our study, we consequently separated our samples into three distinct morphological classes: galaxies in the morphological bin range E-S0 are identified as early-type galaxies (EtG), galaxies in the morphological bin range S0a-Sb are identified as early-type spirals (EtS) and the rest, Sbc and later, are identified as late-type spirals (LtS). In Table 1, we present the statistics for the distribution of morphological classes in our two samples. Clearly, in the HCG sample the fraction of early-type galaxies (both EtG and EtS) is significantly higher than in the CIG sample.

2.5. Luminosity and mass distributions

To compare the physical characteristics of the galaxies in our two samples, we determined the luminosities using the total apparent corrected B-magnitudes compiled in HYPERCAT (Paturel et al. 1994, 1997). These magnitudes were corrected for galactic and internal extinction, and k-correction. This information is missing only for HCG 31q. Moreover, for most of the galaxies in both samples, that is, 80% and 96% of the total HCG and CIG respectively, we extracted the K-band magnitudes at the 20 mag arcsec^{-2} isophote, as compiled in the *2MASS*[3] extended source catalog (Jarrett et al. 2000; Skrutskie et al. 2006). These magnitudes were corrected for galactic extinction (Schlegel et al. 1998), and k-correction following Kochanek et al. (2001). To deduce the masses of the galaxies, we adopted a solar value of $M_{\odot,K} = 3.28$ and used the mass-to-luminosity ratios, M/L, for different morphological types as determined in the K band by James et al. (2008).

In Fig. 2 we compare the HCG and CIG luminosity distributions in B as found in the three morphological classes. In the HCG a small fraction of EtG are more luminous than in the CIG. The EtS on the other hand have similar B-luminosity distributions in both samples, with the HCG showing a slightly higher dispersion than the CIG. The LtS in the HCG show a bimodal distribution, which is not observed in the CIG. This agrees with the study of disk galaxies in HCG performed by Iglesias-Páramo & Vílchez (1998).

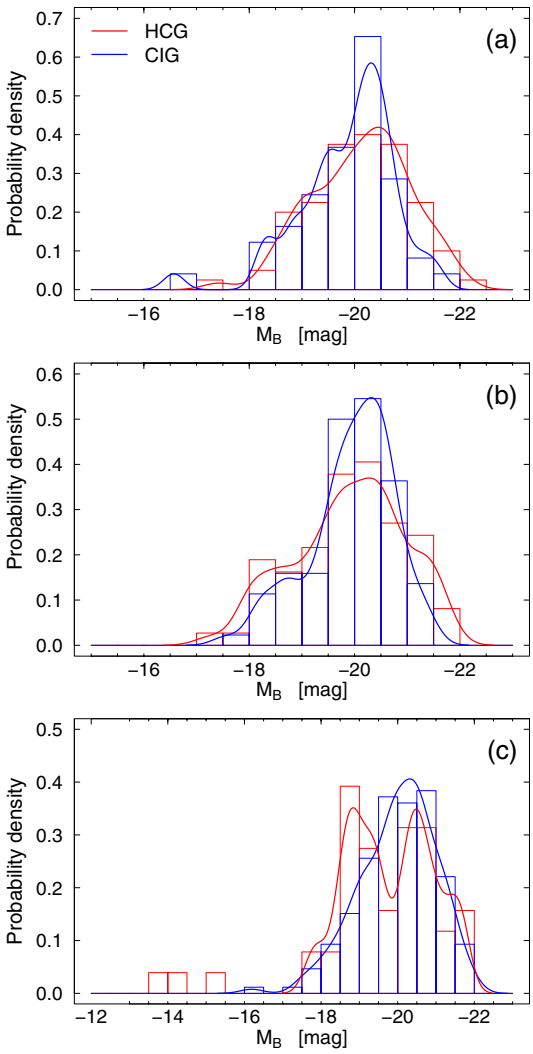

Fig. 2. Comparison of the B-band luminosity distribution in our samples: **a)** early-type galaxies (EtG); **b)** early-spirals (EtS); and **c)** late-spirals (LtS). The continuous curves corresponds to the kernel density estimation of the probability density of each distribution. A Gaussian kernel is used.

In Fig. 3 we show the distributions for the masses. The distributions for the K luminosities are shown as insets in the upper left of the graphics. From these distributions we observe a larger fraction of EtG and EtS in the HCG with higher luminosities, consistent with the assumption that these galaxies are more massive than in the CIG sample.

In Table 2 we present the mean absolute magnitudes of the galaxies in the HCG and CIG samples as measured in the different morphological classes. In the last three columns we report the differences in mean between the two samples, the probability, P, that the difference observed by chance in the sample selection, and the statistical significance, S, of the difference. These values were determined by applying the new parametric ANOVA model introduced by Hothorn et al. (2008) that was developed for the R software by Herberich et al. (2010)[4]. The max-t test takes into account a possible non-normal distribution, unequal variances, and unbalanced sample sizes. The statistical test confirms that the EtG in the HCG are marginally more luminous, and the EtS and LtS show no significant differences.

[3] http://irsa.ipac.caltech.edu

[4] http://www.r-project.org

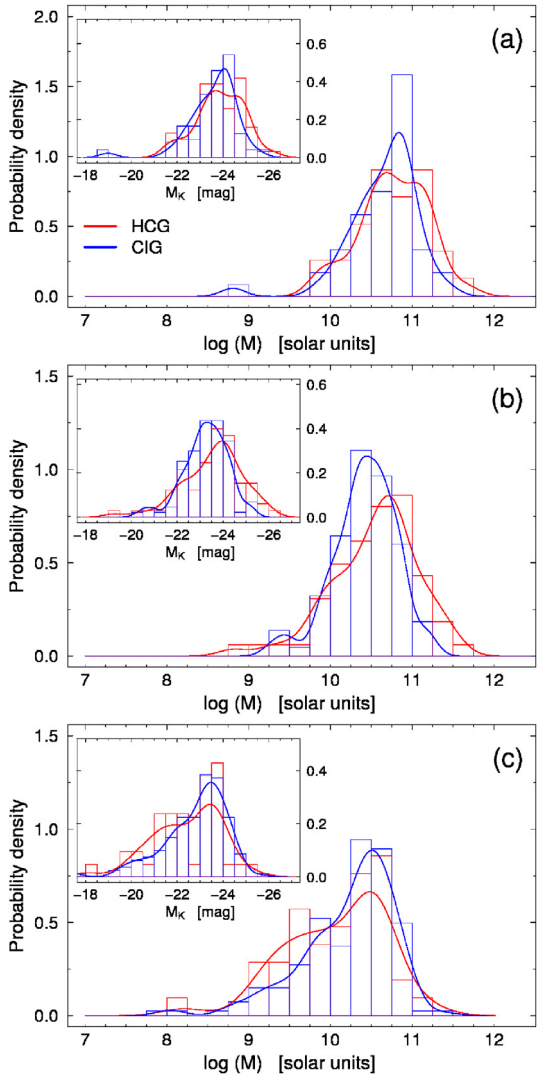

Fig. 3. Comparison of the stellar masses and K-band luminosity (*upper left corners in each panel*) distributions in our samples: **a)** early-type galaxies (EtG); **b)** early-spirals (EtS); and **c)** late-spirals (LtS). The continuous curves corresponds to the kernel density estimation of the probability density of each distribution. A Gaussian kernel is used.

In Table 3 we present the mean absolute magnitudes in the K band and the corresponding mean masses for the HCG and CIG galaxies as measured in the different morphological classes. The results of the max-t test confirm that the EtG and EtS in the HCG are marginally more luminous in the K band and consequently slightly more massive than in the CIG sample. No significant difference is observed for the LtS galaxies.

In Fig. 2 the low-luminosity tail at $M_B \geq -16$ is produced by only three galaxies: HCG 54b, c, and d. Since we did not observe galaxies as weak as these in the rest of our HCG sample or in the CIG sample, we discarded them from our subsequent analyses. Note that according to Verdes-Montenegro et al. (2002), HCG 54 could be the remnant of the merger of two galaxies at an advanced stage of evolution, not a CG.

3. Spectral synthesis analysis method

To determine the SFH, we used the stellar population synthesis code STARLIGHT (Cid Fernandes et al. 2005; Mateus et al. 2006; Asari et al. 2007). Before running STARLIGHT, all spectra in our samples were first corrected for foreground Galactic extinction using the dust maps determined by Schlegel et al. (1998), and then shifted to their respective rest frame. The spectra were also resampled with a spectral step $\Delta\lambda = 1$ Å, within the range 3600 to 7200 Å, and normalized to the median flux of the continuum within the wavelength window 4530 to 4580 Å. STARLIGHT was then run, using a combination of $N_\star$ simple stellar populations (SSP) from the evolutionary synthesis models of Bruzual & Charlot (2003). These models were built based on the medium-resolution Isaac Newton Telescope library of empirical spectra (MILES; Sánchez-Blázquez et al. 2006), following the stellar evolutionary tracks of Padova 1994 (Alongi et al. 1993; Bressan et al. 1993; Fagotto et al. 1994), where the initial mass function (IMF) of Chabrier (2003), and the extinction law of Cardelli et al. (1989) were applied. Our selected base is composed of $N_\star = 150$ SSP, and includes 25 different stellar population ages in the range 1 Myr to 18 Gyr, each with six metallicities. For each galaxy, a mask file was created to exclude spectral ranges around important emission lines ([OII], [NeIII], H_δ, H_γ, H_β, [OIII], HeI, [OI], H_α, [NII], [SII]), the ISM absorption feature (NaD), and bad pixels.

As a result of running STARLIGHT, an optimal continuum template spectrum is produced for each galaxy, from which we can deduce important information about the stellar populations. In this study we concentrate on the SSP fractions at different ages. Following Cid Fernandes et al. (2005), we derived the light-weighted average ages, $\langle \log t_\star \rangle_{\rm L}$, and the mass-weighted average ages, $\langle \log t_\star \rangle_{\rm M}$, which are respectively equal to

$$\langle \log t_\star \rangle_{\rm L} = \sum_{j=1}^{N} x_j \log t_j; \qquad \langle \log t_\star \rangle_{\rm M} = \sum_{j=1}^{N} \mu_j \log t_j, \qquad (1)$$

where $x_{\rm j}$ ($j = 1, ..., N_\star$) are the fractional contributions to the model flux weighted by light of the SSP with ages t_j, and μ_j are the mass fractional contributions obtained by using the model light-to-mass ratios at the normalization λ_0. The SFH is obtained by tracing the population vector x_j or μ_j as a function of t_j. The uncertainties on these values are about ~0.03 dex. This was determined empirically by running STARLIGHT 50 times on nine spectra with different S/N.

By definition, the two weighted average ages are sensitive to different stellar populations: $\langle \log t_\star \rangle_{\rm L}$ is sensitive to the presence of young stellar populations because of their higher contribution in light, while $\langle \log t_\star \rangle_{\rm M}$ is sensitive to the less luminous and older stellar populations, which form the bulk of galaxy mass. Considering that the uncertainties in both average ages are of the same order, a quantitative estimate of the star formation time scale (SFTS) activity in each galaxy can be obtained by calculating the difference of mass-weighted and light-weighted average stellar ages as

$$\Delta(t_\star) = 10^{\langle \log t_\star \rangle_{\rm M}} - 10^{\langle \log t_\star \rangle_{\rm L}} \quad \text{(in Gyr)}. \qquad (2)$$

Table 2. Luminosities in B band.

Morph. class	M_B (mag) HCG	M_B (mag) CIG	$\Delta M_B \pm \sigma$ (mag)	P	S^a
EtG	−20.1	−19.9	0.25 ± 0.17	0.14	1.5σ
EtS	−19.9	−19.9	0.05 ± 0.15	0.75	...
LtS	−19.9	−20.0	0.13 ± 0.18	0.46	...

Notes. [(a)] Values $\leq 1\sigma$ are not shown.

Table 3. Luminosities in K band and corresponding masses.

Morph. class	M_K (mag)		$\Delta M_K \pm \sigma$ (mag)	$\log(M/M_\odot)$		$\Delta \log(M/M_\odot) \pm \sigma$	P	S^a
	HCG	CIG		HCG	CIG			
EtG	−23.9	−23.6	0.30 ± 0.21	10.8	10.6	0.12 ± 0.08	0.15	1.5σ
EtS	−23.5	−23.5	0.30 ± 0.20	10.5	10.4	0.12 ± 0.08	0.13	1.5σ
LtS	−22.5	−22.8	0.26 ± 0.24	10.1	10.2	0.11 ± 0.10	0.27	...

Notes. [(a)] Values $\leq 1\sigma$ are not shown.

For example, a galaxy that experienced constant star formation over its lifetime, a typical late-type spiral galaxy, would be expected to have a long $\Delta(t_\star)$, the value growing with time. On the other hand, an early-type galaxy, a typical elliptical galaxy for example, where star formation has stopped long ago, would be expected to have a short $\Delta(t_\star)$, the value decreasing with time. Note that a very young star-forming galaxy would also have a short $\Delta(t_\star)$, but this is because both light and mass are dominated by young stars, and the value would be expected to increase with time. More important, different $\Delta(t_\star)$ for the same morphology and mass in different environments could indicate special formation conditions, which is exactly what our present study looks for.

Following Cid Fernandes et al. (2001, 2005), we calculated the light (x_j) and mass-weighted (μ_j) population vectors in three different age groups: young (Y), with ages in the range $t \leq 10^8$ yr (the vectors are identified as X_Y and M_Y for light-weight and mass-weight, respectively), intermediate (I), with ages within the range $10^8 < t < 5 \times 10^9$ yr (identified as X_I and M_I), and old (O) with stellar population ages in the range $t \geq 5 \times 10^9$ yr (identified as X_O and M_O). For each weighted population vector, we then determined the percentage contribution in the three age groups.

To illustrate our method, we show in Fig. 4 the results of applying STARLIGHT to two different galaxies in our samples: an early-type isolated galaxy, CIG 257, and a late-type galaxy in CG, HCG 49b. In Fig. 4a it can be seen that in this early-type galaxy the old stellar populations dominate both in light and mass (i.e. the highest values are those in X_O and M_O). On the other hand, in the late-type spiral (Fig. 4b), the young stellar populations dominate the light (i.e. the largest is X_Y and then X_I), while a mixture of stars of old and intermediate stellar ages dominate the mass (i.e. M_O and M_I are comparable).

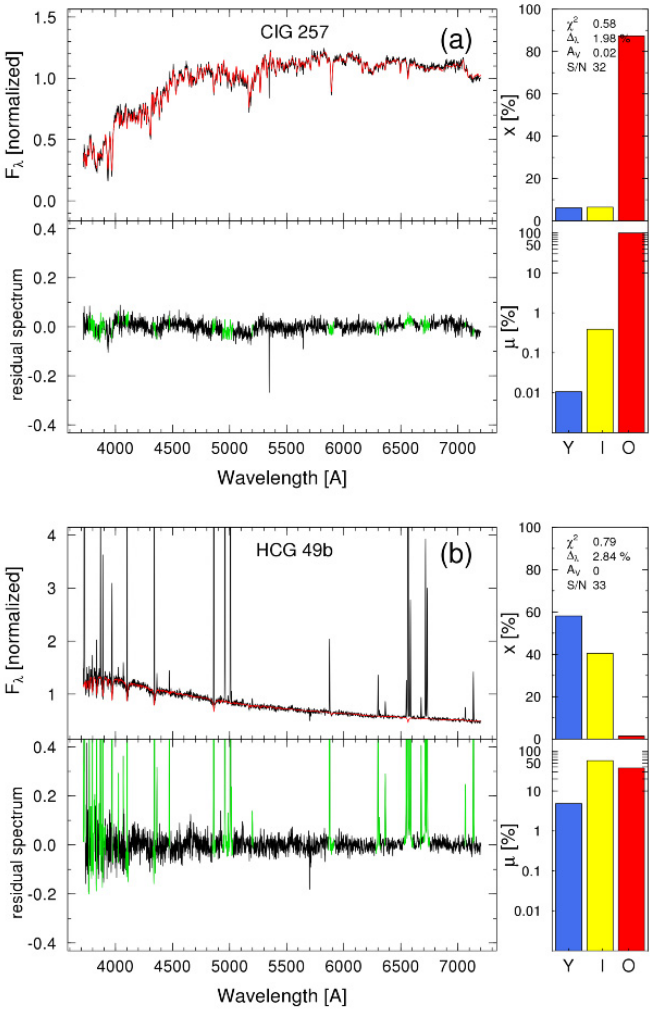

Fig. 4. Spectral synthesis results for two galaxies in our samples. **a)** An early-type galaxy, CIG 257; and **b)** a late-type galaxy, HCG 49b. The *top-left plot* in each panel shows the synthetic spectrum (red curve), plotted over the observed spectrum (black curve) normalized by the flux at $\lambda = 4550$ Å; the *bottom-left plot* shows the residual spectrum (the difference between the observed and the synthetic continuum spectra), with the green regions representing the mask used; the *top-right plot* shows the percentage contribution of the light-weighted population vector (x[%]), and the *bottom-right plot* the percentage contribution of the mass-weighted population vector (μ[%] in logarithmic scale), as calculated in each of the three different SSP age groups: young (blue bar), intermediate (yellow bar), and old stellar population bins (red bar).

4. Results

As explained in Sect. 2.4, we separated our two samples into three morphological classes: early-type galaxies (EtG), early-type spirals (EtS), and late-type spirals (LtS). In Figs. 5 we show the percentage contribution of the mass-weighted (Mw) population vectors of each age group as found in the different morphological classes. In Fig. 6 we show the percentage contribution of the light-weighted (Lw) vectors. In each graph, we have traced the confidence interval model (gray area) constructed by assuming that the two samples come from the same distribution. The corresponding mean values of the distributions, the difference between means, and the statistical significance given by the statistical tests are reported in Tables 4 and 5 for the Mw and Lw population vectors, respectively.

The distributions of the Mw and Lw average stellar ages for each morphological class are shown in Figs. 7 and 8, respectively. The mean values of the distributions are reported in Table 6. As mentioned in Sect. 3, by studying the difference between the two average ages, $\Delta(t_\star)$, it is possible to quantify the SFTS of the galaxies. Low values of SFTS indicate that both mass and light are produced by the same type of stars, which implies that galaxies must have formed all their stars at roughly

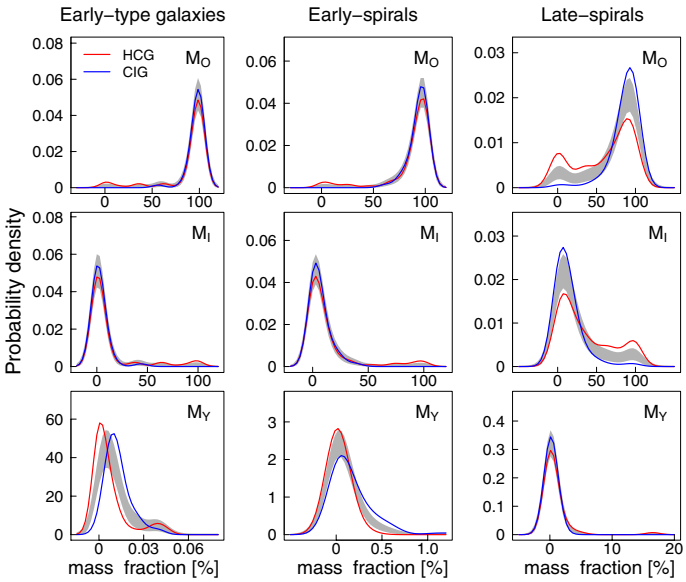

Fig. 5. Percentage contribution of the mass-weighted population vectors (*top to bottom*) M_O, M_I, and M_Y, as measured in the different morphological classes, (*left to right)* EtG, EtS, and LtS galaxies. The red and blue curves are the density distributions for the HCG and CIG, respectively. The gray areas are the confidence interval models, assuming the two samples come from the same distribution. In each graph the curves are the continuous representation of the distribution. These curves were produced using the SM function in the R statistical package.

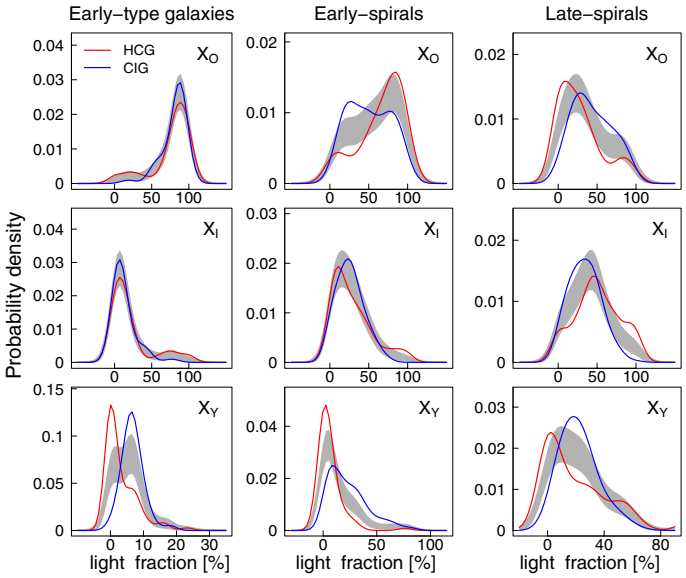

Fig. 6. Same as Fig. 5 for the light-weighted population vectors.

Table 4. Mean values of the mass-weighted population vectors.

Population vector	μ [%] HCG	μ [%] CIG	$\Delta\mu \pm \sigma$ [%]	P	S^a
		EtG			
M_O	88.4	97.0	8.6 ± 3.2	0.007	2.7σ
M_I	11.6	2.9	8.6 ± 3.2	0.007	2.7σ
M_Y	0.007	0.013	0.006 ± 0.002	0.003	3.1σ
		EtS			
M_O	86.7	93.6	6.9 ± 2.9	0.019	2.4σ
M_I	13.3	6.2	7.0 ± 2.9	0.017	2.4σ
M_Y	0.06	0.19	0.13 ± 0.05	0.008	2.7σ
		LtS (old)			
M_O	89.4	91.3	1.9 ± 1.8	0.30	...
M_I	10.4	8.6	1.8 ± 1.8	0.30	...
M_Y	0.16	0.16	0.00 ± 0.04	0.92	...
		LtS (young)			
M_O	27.8	44.4	16.6 ± 8.0	0.04	2.1σ
M_I	62.5	54.8	7.7 ± 8.7	0.38	...
M_Y	9.7	0.8	9.0 ± 5.8	0.13	...

Notes. [(a)] Values $<2\sigma$ are not shown.

Table 5. Median values of the light-weighted population vectors.

Population vector	x [%] HCG	x [%] CIG	$\Delta x \pm \sigma$ [%]	P	S^a
		EtG			
X_O	75.8	80.6	4.9 ± 3.9	0.22	...
X_I	21.0	12.6	8.4 ± 4.0	0.04	2.1σ
X_Y	3.2	6.7	3.5 ± 0.7	10^{-6}	4.8σ
		EtS			
X_O	65.1	50.8	14.3 ± 4.4	0.001	3.3σ
X_I	28.9	25.8	3.2 ± 3.5	0.36	...
X_Y	5.9	23.0	17.5 ± 2.4	10^{-11}	7.4σ
		LtS (old)			
X_O	45.9	47.5	1.6 ± 5.8	0.79	...
X_I	34.4	30.5	3.8 ± 4.1	0.35	...
X_Y	20.0	22.0	2.3 ± 3.9	0.56	...
		LtS (young)			
X_O	9.8	9.6	0.3 ± 3.8	0.94	...
X_I	66.3	66.2	0.1 ± 7.1	0.99	...
X_Y	24.0	24.0	0.3 ± 7.7	0.97	...

Notes. [(a)] Values $<2\sigma$ are not shown.

the same time. The SFTS, therefore, is an indicator of how fast a galaxy created its stellar population, or how long the stellar activity was prolonged in this galaxy. In Table 7 we present the mean values of the SFTS and the statistical significance produced by the statistical tests by comparing these values in the two samples. In the following subsections we discuss the results individually for each morphological class.

4.1. Early-type galaxies (EtG)

The final number of galaxies in this morphological class is 79 in the HCG and 43 in the CIG sample. We discarded seven EtG, one in the HCG and six in the CIG sample, because we consider them to be atypical for their morphology. The nature of the peculiarity observed in these galaxies is discussed briefly in Sect. 4.1.1. Here, we present the results of what we consider the typical EtG in both samples.

As can be seen in the left panels of Fig. 5 and 6 for the *Mw* and *Lw* vectors, respectively, old stellar populations dominate the mass ($M_O \sim 90\%$) and light ($X_O \sim 80\%$) in EtG galaxies in both samples. In the HCG there is a small fraction of galaxies showing low M_O and high M_I values. This explains the differences observed in Tables 4 and 5. However, the difference in X_O vector is not statistically significant. The most important difference observed between the stellar population vectors in the two samples is the lower contribution of young stellar populations in the HCG. This difference is statistically significant for both the *Mw* and *Lw* vectors.

In Figs. 7a and 8a we show the distributions for the *Mw* and *Lw* average stellar ages, respectively. The mean values are

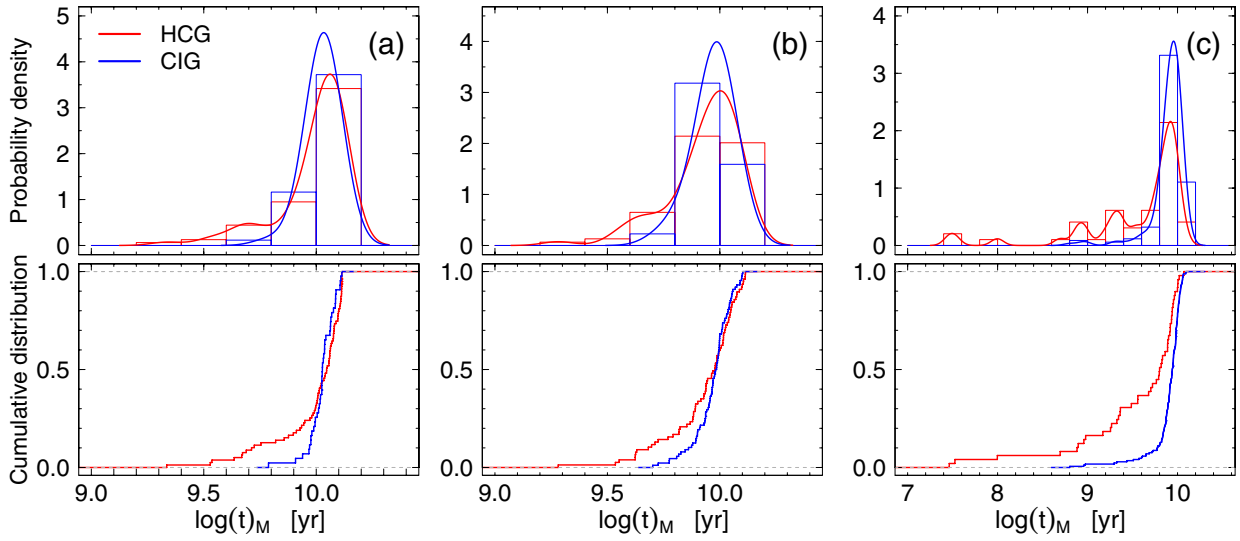

Fig. 7. Histogram and cumulative distribution of mass-weighted average stellar ages in the three morphological classes: **a)** EtG; **b)** EtS; and **c)** LtS galaxies.

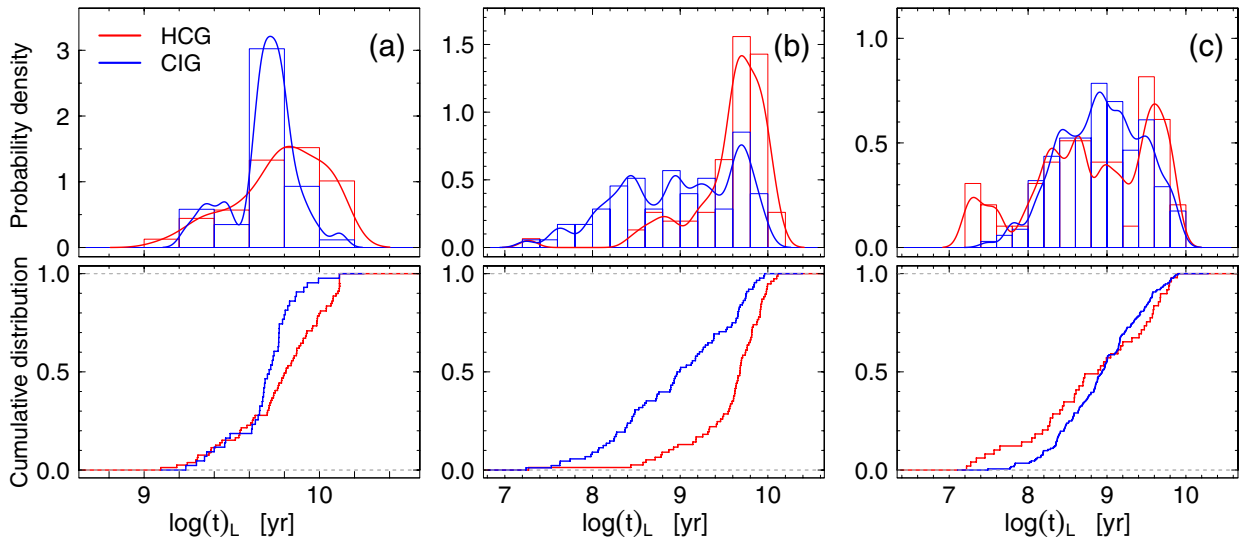

Fig. 8. Histogram and cumulative distribution of light-weighted average stellar ages in the three morphological classes: **a)** EtG; **b)** EtS; and **c)** LtS galaxies.

Table 6. Light-weighted and mass-weighted average stellar ages.

Morphological	Number		$\langle t_\star\rangle_{\rm L}^{a}$		$\Delta\langle t_\star\rangle_{\rm L} \pm \sigma$	P	S^c	$\langle t_\star\rangle_{\rm M}^{b}$		$\Delta\langle t_\star\rangle_{\rm M} \pm \sigma$	P	S^c
class	HCG	CIG	HCG	CIG				HCG	CIG			
EtG	79	43	6.0	4.9	1.2 ± 0.6	0.04	2.0σ	9.7	10.7	1.1 ± 0.6	0.06	...
EtS	77	88	3.7	0.9	4.0 ± 0.6	2×10^{-10}	6.8σ	8.5	9.3	1.1 ± 0.5	0.04	2.1σ
LtS (old)	25	155	0.9	0.9	$\sim$0.1	0.99	...	7.6	8.8	1.2 ± 0.5	0.02	2.4σ
LtS (young)	24	17	0.4	0.3	0.1 ± 0.4	0.73	...	1.2	3.0	2.4 ± 1.1	0.03	2.2σ

Notes. All ages are in units of Gyr. $^{(a,b)}$ These values correspond to the geometric mean of the galaxy ages in each morphological class (i.e. $10^{\langle \log t_\star\rangle_{\rm L}}$ and $10^{\langle \log t_\star\rangle_{\rm M}}$). $^{(c)}$ Values $<2\sigma$ are not shown.

reported in Table 6. The EtG in the HCG galaxies are found to be slightly older than in the CIG, when the *Lw* vectors are considered ($\langle t_\star\rangle_{\rm L}$), while no difference is detected when the *Mw* vectors are considered ($\langle t_\star\rangle_{\rm M}$).

To put the results of our analysis in a more comprehensive form, we trace in Fig. 9 the SFTS, namely $\langle t_\star\rangle_{\rm M}$ vs. $\Delta(t_\star)$. In each graph we also show $\langle t_\star\rangle_{\rm L}$ as a color-code bar and we distinguish among different morphological types using different symbols. In Fig. 9 we see that most of the EtG in both samples have $\langle t_\star\rangle_{\rm L}$ between 4 to 9 Gyr (from green to orange), with a clear tendency for HCG to be older than the CIG in this morphological class, this is regardless of the morphological types. In particular, we find in the HCG a significant number of very old galaxies, mostly E-E/S0, but also including some S0, all with $\Delta(t_\star)$ remarkably short ($\lesssim$3 Gyr) and only one EtG in the CIG below this values. This difference is consistent with longer SFTS

Table 7. Mean star formation activity time scales (SFTS).

Morphological class	$\langle\Delta(t_\star)\rangle$ HCG	CIG	$\Delta \pm \sigma$	P	S
EtG	3.3	5.4	2.1 ± 0.4	1×10^{-7}	5.6σ
EtS	3.8	7.3	3.5 ± 0.4	4×10^{-16}	9.1σ
LtS (old)	5.7	7.3	1.6 ± 0.6	0.009	2.6σ
LtS (young)	1.2	3.1	1.8 ± 0.5	0.001	3.6σ

Notes. All ages are in units of Gyr.

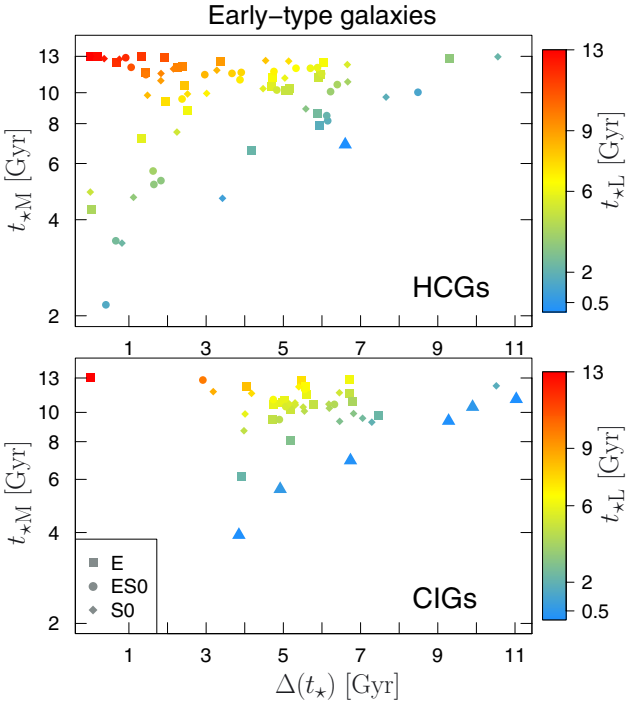

Fig. 9. Star formation activity time scale traced in terms of mass-weighted age $t_{\star\,\mathrm{M}}$ as a function of $\Delta(t_\star)$ for EtG in HCG sample (*top panel*) and the CIG sample (*bottom panel*). The color-code bar corresponds to light-weighted age $t_{\star\,\mathrm{L}}$. Triangles represent the peculiar galaxies.

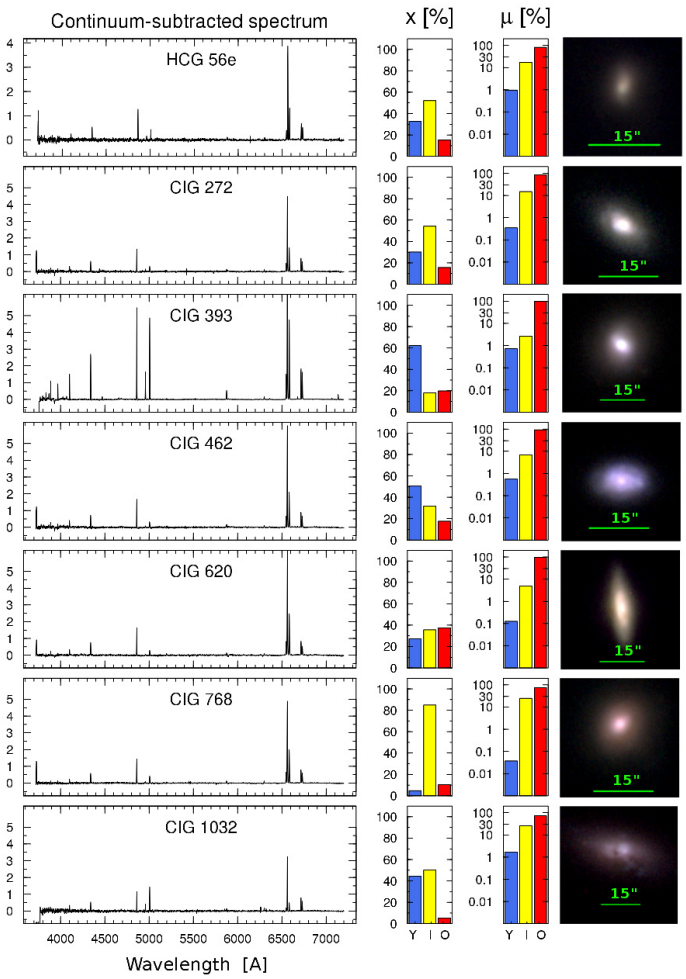

Fig. 10. Spectral synthesis results for the seven peculiar EtG. *Left panels*: continuum-subtracted spectra showing the presence of strong emission lines; *middle panels*: percentage contribution of the *Lw* and *Mw* population vectors; *right panels*: *gri* composite SDSS images. In these galaxies, the X_I and/or X_Y stellar populations tend to dominate the light, which is not typical of EtG.

for the galaxies in the CIG than in the HCG. The statistical tests reported in Table 7 confirm this difference: in the HCG the galaxies have less prolonged SFTS by ∼2 Gyr than their counterparts in the CIG sample.

The above differences are consistent with slightly different formation processes for the galaxies in the different environments. In the HCG the EtG have formed their stars over shorter time scales than similar galaxies in isolation. This result is similar to those obtained by Proctor et al. (2004), Mendes de Oliveira et al. (2005) and de la Rosa et al. (2007) for elliptical galaxies in CG. This is also a recognized characteristic of early-type galaxies forming in clusters of galaxies (Balogh et al. 1999; Thomas et al. 2005; Bernardi et al. 2006; Gobat et al. 2008; Clemens et al. 2009; Cooper et al. 2010; Hoyle et al. 2011).

4.1.1. Nature of peculiar EtG

The seven EtG discarded form the previous analysis due to their atypical spectra for this morphological class are HCG 56e, CIG 272, CIG 393, CIG 462, CIG 620, CIG 768, and CIG 1032. In Fig. 10 we show the residual optical spectra, the population vector analysis and the morphology of these galaxies. In the middle panels of Fig. 10 we see that although the M_O vectors are dominant, the X_I and X_Y are the highest, suggesting intermediate or young stellar populations are producing the light, which is consistent with recent star formation episodes. Indeed, the residual spectra in the left panel of Fig. 10 show intense emission lines consistent with a star formation activity (as determined based on a standard diagnostic diagram; Baldwin et al. 1981).

As an independent test, we also determined the near-UV minus optical color (NUV-r) for these galaxies (Yi et al. 2005; Schawinski et al. 2007), taking the NUV (λ2270 Å) magnitudes from the *GALEX* extended source catalog (Martin et al. 2005), and the r magnitudes from the SDSS r-band Petrosian magnitudes. The NUV-r colors range from 3.1 in CIG 272 to 4.0 in CIG 620 (HCG 56e has 3.2), which is consistent with very young ($\lesssim$1 Gyr) stellar populations (Yi et al. 2005; Schawinski et al. 2007).

The images in SDSS in Fig. 10 give no obvious clue why these EtG show evidence of recent star formation activity. In particular, we detect no trace of interaction. However, according to Thomas et al. (2010), evidence of recent star formation in EtG is a common phenomenon. These authors also suggested that the fraction of EtG showing current star formation (they call it the "rejuvenation fraction") in low-density environments is 10%

higher than in high-density ones, which suggests that they are generated by internal processes. Taken at face value, this seems to agree with what we observe, counting 6 out of 49 (12%) such galaxies in the CIG compared to only 1 out of 80 in the HCG sample.

Alternatively, some of these galaxies may have been misclassified morphologically. According to Bitsakis et al. (2011) for example, HCG 56e could be a dusty obscured late-type galaxy. We can vaguely see some spiral structures in some of the galaxies in Fig. 10 (although not in the optical images of HCG 56e). Dust seems also to be present, but this is more a normal characteristic of star-forming regions than an indicator of a late-type morphology.

In Fig. 9, the peculiar EtG were included as blue triangles. In the CIG sample these galaxies trace a sequence where $\langle t_\star \rangle_M$ increases almost linearly with $\Delta(t_\star)$, which is consistent with constant star formation. The fact that this sequence is similar to the one displayed by the EtS and LtS in our sample, as we will show in Sects. 4.2 and 4.3, reinforced the argument that suggests that these could be misclassified late-type galaxies.

4.2. Early-type spirals (EtS)

We count 77 EtS in the HCG compared to 88 in the CIG samples. Because both samples have a comparable fraction of these galaxies (see Table 1) in contrast it is clear that to the EtG, the EtS show no special preference to form in dense environments.

In the middle panels of Figs. 5 and 6 we show the distributions of Mw and Lw stellar population vectors, respectively, for each age group. In Tables 4 and 5 we report the mean values of these distributions, the difference between means, and the statistical significance determined by the statistical tests. In Fig. 5 it can be seen that the distribution of the old and intermediate stellar population vectors, M_O and M_I, in both samples are similar. Only a small fraction of galaxies in the HCG have lower values of M_O and higher values of M_I, like observed in the EtG. Again, like for the EtG, the distributions for the young stellar population vectors, M_Y, are those that differ more drastically comparing the two samples. We observe lower values of M_Y and X_Y in the HCG than in the CIG. From the Lw vectors, we deduce that the galaxies in the HCG have higher values of X_O and lower values X_Y than in the CIG (no significant difference is observe for X_I). The EtS in the HCG are therefore dominated by older stellar populations than in the CIG and are clearly deficient in young stellar populations.

Except for the small fraction of galaxies in the HCG with strong contribution from intermediate age populations, which produce slightly younger ages in $\langle t_\star \rangle_M$, the distributions of Mw average stellar ages in Fig. 7b are comparable in the two samples. This result is similar to the one obtained for the EtG. Once again, the most remarkable difference appears for the Lw average ages, $\langle t_\star \rangle_L$. In the HCG, the EtS are older that in the CIG (cf. Fig. 8b and Table 6). The difference seems even higher than what we observed for the EtG, the galaxies in the HCG looking older than in the CIG by as much as ∼4 Gyr. Also noted in Fig. 8b is the dispersion in age, which is much narrower in the HCG than in the CIG sample.

Once again, these differences become easier to understand by considering the SFTS. In Fig. 11 we observe the same difference as before for the EtG. In the HCG, the EtS are older than in the CIG and most of them have low values of $\Delta(t_\star)$, which is not observed in the CIG sample. The EtS in the HCG have lower SFTS than similar galaxies in isolation, indicating that these galaxies in compact groups have a shorter star formation

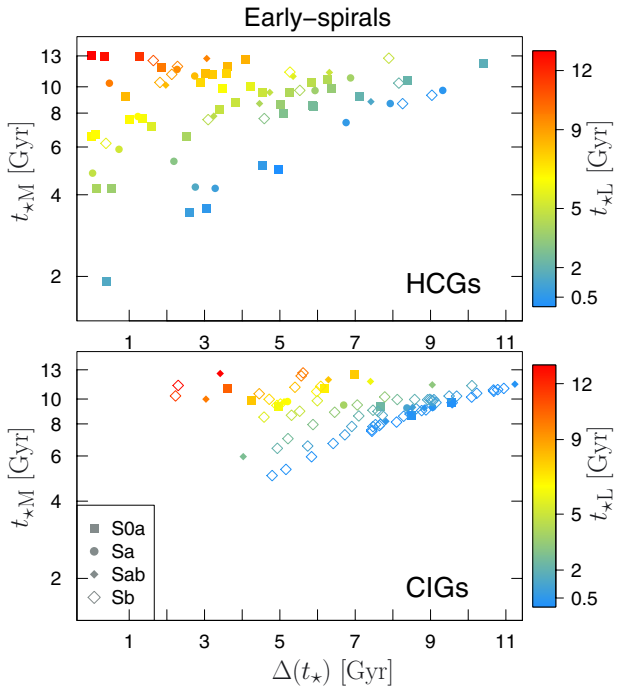

Fig. 11. Same as Fig. 9 for EtS galaxies.

activity. This is confirmed by the statistical tests presented in Table 7, where we find on average an SFTS shorter by about 3 Gyr in the HCG than in the CIG and we do not distinguish any trend with the morphological type.

4.3. Late-type spirals (LtS)

In this morphological class we find again a large difference in the number of galaxies between the two samples. We count only 49 LtS in the HCG compared to 172 in the CIG sample. Clearly, galaxies in isolation are mostly late-type spirals. This is an important difference that must be taken into account. Whatever the processes acting in CG, these are related to a change toward earlier-type morphologies.

In the right panels of Figs. 5 and 6 we present the percentage contribution of the Mw and Lw stellar populations, respectively, for the LtS in our two samples. In contrast to the CIG, the distribution of M_O in the HCG (Fig. 5) presents a bimodal distribution. A considerable fraction of LtS in the HCG has values $M_O < 70\%$, which means that they formed up to 70% of their stars during the last 5 Gyr. This low fraction of M_0 is found in 49% of the LtS in the HCG galaxies (24 out of 49) compared to only 10% (17 out of 172) of CIG. To take this important difference between the two samples into account, we separated our samples of LtS galaxies into two subclasses: LtS with $M_O > 70\%$ are classified as old, and those that do not meet this criterion are classified as young. In Tables 4 and 5 we present separately the mean values of the Mw and Lw population vectors for old and young LtS. Moreover, in Table 6 we report for the average stellar ages the mean values of the distributions, the differences between the means, and the statistical significance of the differences between the samples.

The presence of the young LtS in the HCG explains the differences observed in Figs. 5 and 6. No significant differences are observed in Table 4 (except for an even smaller M_O in the young LtS in HCG than in the CIG sample) and Table 5 when the distinction between young and old LtS is taken into account. The presence of the young LtS in the HCG also explains the

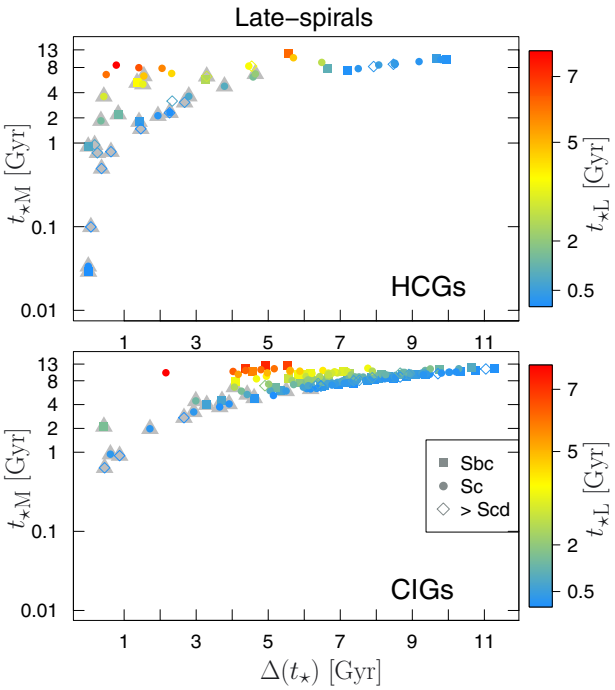

Fig. 12. Same as Fig. 9 for LtS galaxies. Young LtS galaxies in the samples are indicated with gray triangles.

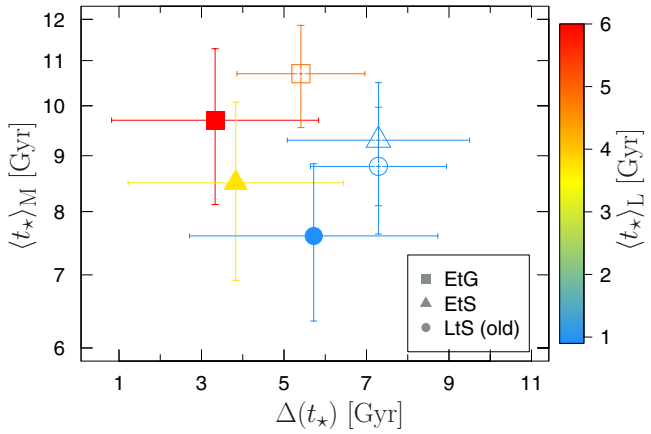

Fig. 13. Mean SFTS for EtG, EtS, and old LtS galaxies in HCG (filled symbols) and CIG samples (open symbols). Error bars are $\pm\sigma$ of the mean values.

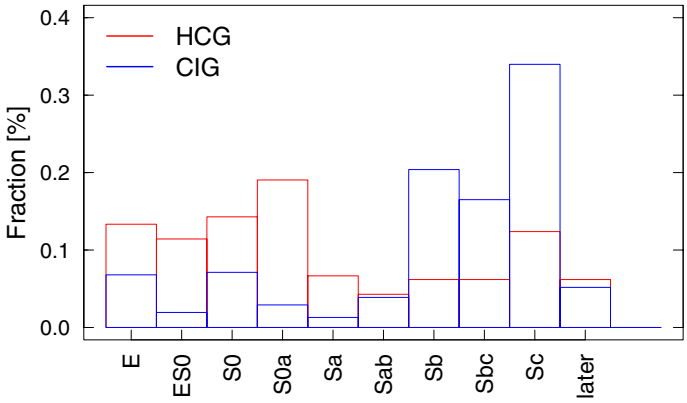

Fig. 14. Morphology type distribution of galaxies in the HCG and CIG samples.

younger *Mw* average stellar ages in Fig. 7c, which is confirmed in Table 6. Most of the young LtS are smaller in size than the old LtS, with a median value in diameter at 25 mag arcsec^{-2} isophote of D_{25} = 15 kpc, both in the HCG and CIG samples (for the old LtS this value is ∼24 kpc) and have masses of about $\log(M/M_\odot) < 10$. Interestingly, we found that 50% of the young LtS belong to compact groups in which most of the members are also LtS. These are HCG 31a, b, c, g, q, HCG 49a, b, c, d, and HCG 100b, c, d. These galaxies have a median value of $\langle t_\star \rangle_L \sim 200$ Myr, which confirms that they are possible examples of very young groups, as was previously suggested in the literature (Iglesias-Páramo & Vílchez 1997; Vílchez & Iglesias-Páramo 1998; Verdes-Montenegro et al. 2005; de Mello et al. 2008; Torres-Flores et al. 2010).

In Fig. 12 we show the SFTS for the LtS and report the mean values in Table 7. Here we have to be careful in interpreting the results. The young LtS in the HCG have a short $\Delta(t_\star)$ (gray triangles in Fig. 12), mainly because they show young ages with roughly similar values of $\langle t_\star \rangle_M$ and $\langle t_\star \rangle_L$, which is consistent with very young star-forming galaxies. The old LtS on the other hand show the same trend as observed before for the EtG and EtS morphological classes, with an SFTS shorter in the HCG than in the CIG by almost 2 Gyr.

5. Discussion and conclusions

To summarize our analysis, we show in Fig. 13 the mean SFTS as measured in the three morphological classes, EtG, EtS and LtS (old subclass only), comparing the HCG with the CIG. The most remarkable difference observed between the galaxies in the HCG (filled symbols) and CIG (open symbols) is the shorter star formation activity, namely SFTS, in the HCG compared to the CIG sample. The SFTS is shorter by ∼2 Gyr in the EtG and LtS, and even shorter by ∼3.5 Gyr in the EtS. These differences are independent of the morphology, mass, and luminosity of the galaxies.

For the EtG, we conclude that they have formed their stars more rapidly. In other words, our results suggest that the EtG in the HCG show higher astration rates than in the CIG (i.e., they transformed their gas more efficiently into stars). Higher astration rates for the EtG imply more frequent mergers (Coziol et al. 2011). This is consistent with the hierarchical galaxy formation model, according to which gas-rich protogalaxies in dense environments experience more frequent mergers, producing galaxies with earlier-type morphologies (i.e., galaxies with bigger bulges). However, since the CG are forming from lower-mass density fluctuations than clusters of galaxies, very few of these mergers would produce massive elliptical galaxies. This picture is consistent with the morphological distribution in the HCG, as seen in Fig. 14, which shows that these systems are dominated by lenticular galaxies.

For the EtS and LtS, the interpretation is not as obvious as for the EtG. In these galaxies, we cannot eliminate a priori tidal gas stripping as a possible mechanism to reduce the SFTS. These would be examples of galaxies that fell into the CG later. To test the gas-stripping hypothesis, we calculated the specific star formation rate (SSFR) of all spiral galaxies in our samples (EtS and LtS galaxies). The SSFR, defined as the actual SFR divided by the stellar mass, reflects the mass of stars formed during the last 10^8 yr. The SSFR is estimated using STARLIGHT by integrating the mass-weighted population vector over the young age group M_Y (see Eq. (6) in Asari et al. 2007). In Fig. 15a we compare the distributions of the SSFR in the HCG and CIG samples. The distribution of SSFR is clearly bimodal (i.e. with a gap) for the

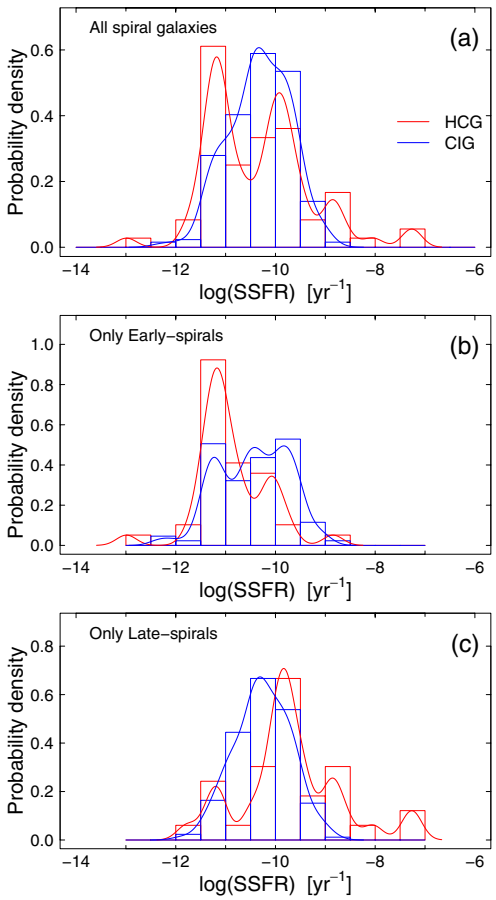

Fig. 15. Comparison of the distributions of SSFR in the samples: **a)** both EtS and LtS; **b)** only EtS; and **c)** only LtS galaxies.

HCG, while the distribution of the CIG is continuous. The bimodal distribution of the HCG is a by-product of a difference in morphology. As before, we distinguish between early- and and late-type spirals in both samples and find that the EtS in the HCG have a distribution of SSFR that peaks at lower values than for the CIG distribution (Fig. 15b). On the other hand, the SSFR of the LtS in HCG peaks at a higher value than in the CIG sample (Fig. 15c). This is consistent with the hypothesis that late-type spirals, still rich in gas, are recent acquisitions in CG. By falling into the group, these galaxies increase their star formation and rapidly consume their gas (i.e., higher astration rates). Thus, by increasing their astration rates and interacting with other galaxies, these new members will transform into earlier-type spirals. Note that this interpretation does not eliminate tidal gas stripping completely, which surely may also play a role in lowering the SFTS of these galaxies. However, our test indicates that this is not the main mechanism. Recent studies, based on UV and IR data, have also found a bimodality (gap) in the distribution of SSFR in HCG galaxies and suggested that the high-density environment of CGs has accelerated the evolution of galaxies, transforming star-forming galaxies into quiescent galaxies (Johnson et al. 2007; Tzanavaris et al. 2010; Walker et al. 2010; Bitsakis et al. 2010, 2011).

According to our analysis, galaxies in the HCG have shorter SFTS than in the CIG because they have experienced higher astration rates. This explains why galaxies in HCG are generally deficient in gas (Williams & Rood 1987; Verdes-Montenegro et al. 2001; Borthakur et al. 2010). The galaxies evolved more rapidly than in the field. This is consistent with the hierarchical galaxy formation model, which states that CG are structures that formed recently from primordial low fluctuations in mass density. As for the time of the formation of the HCG, the systematic difference in SFTS suggests this could have happened 2 to 3.5 Gyr in the past.

Our observations reinforce the idea that these are examples of relatively young structures, as has been discussed by Hickson (1997, and references therein). However, ∼3 Gyr for the time of formation of these structures may still seem too old to explain why these systems have not collapsed into more gravitationally bound objects, such as a giant blue elliptical galaxy (indeed, dynamically speaking, we should have rather expected a smaller version of a cD galaxy, i.e. an elliptical galaxy with an inflated envelope). In the introduction, we have briefly mentioned why such a final state for the HCG is not plausible according to the hierarchical galaxy formation model. This is because these structures formed from very small density fluctuation regions, which had not enough mass to transform gas-rich protogalaxies into giant elliptical or cD galaxies.

Does this mean that the HCG must be in some sort of dynamical equilibrium? This hypothesis was tested by Plauchu-Frayn & Coziol (2010a,b), who showed that galaxies in the HCG are not in an equilibrium state, but are merging without gas. Now, it is worth emphasizing the main dynamical consequence of the absence of gas on mergers. By definition, gravity is a conservative force, which implies that to form a gravitationally bounded structure, a system must loose some of its energy. This is where the presence of free gas plays a key role. The interaction of gas-rich protogalaxies is a highly dissipative process. The gas is heated, then cooled through radiation, and nonisotropic gravitational interactions produce gas turbulence, which induces star formation and triggers the formation of SMBH at the center of galaxies. Therefore, the first phase in the formation of galaxies in CG must be relatively fast, because of the high level of dissipation of energy produced by the gas. This is consistent with the short SFTS found in HCG and the bimodality in the SSFR distribution. However, subsequent interactions between gas-poor galaxies (i.e., dry mergers) are a much less dissipative process, and consequently the dynamical time scales for the merger of these systems may be longer than initially assumed (a few Gyr), which would explain why we still observe CG in their present states.

To summarize, our analysis reveals that the galaxies in the HCG are older than in the CIG and that their SFTS are shorter by ∼3 Gyr. Considering that these are systematic differences, independent of the morphology, of the mass, and of luminosity of the galaxies, we conclude that this can only imply that the galaxies in the HCG formed their stellar population faster than the galaxies in the CIG. We conclude that the main effect of the environment on galaxies in the HCG sample is an increase of astration rate, consistent with the fast mergers of gas-rich protogalaxies. This is consistent with the hierarchical galaxy formation model, which states that the HCG are relatively recent structures that formed from primordial low-mass density fluctuations. Based on the systematic difference in SFTS, we propose that the HCG most probably formed ∼3 Gyr in the past. The galaxies in the HCG are not in equilibrium but are merging without gas, which may explain why they have a longer dynamical lifetime.

Acknowledgements. We are grateful to M. A. Martínez for making available her sample of HCG spectra and to J. Perea, C. Husillos, and J. Islas-Islas for useful comments on this work. I. P.-F. acknowledges the postdoctoral fellowship grants 145727 and 170304 from CONACyT Mexico and partial support from the Spanish research project AYA2010-15196. A.d.O. is partially supported by the Spanish research project AYA2010-22111, Junta de Andalucía TIC114 and

the Excellence project P08-TIC-3531. T.-P. acknowledges PROMEP for support grant 103.5-10-4684 and DAIPGto (0065/11). We thank the anonymous referee for the valuable and detailed comments that improved this manuscript. Finally, we acknowledge the use of the following databases and software. Funding for the Sloan Digital Sky Survey (SDSS) has been provided by the Alfred P. Sloan Foundation, the Participating Institutions, the National Aeronautics and Space Administration, the National Science Foundation, the US Department of Energy, the Japanese Monbukagakusho and the Max-Planck Society. The SDSS is managed by the Astrophysical Research Consortium for the participating Institutions. The Participating Institutions are the University of Chicago, Fermilab, the Institute for Advanced Study, the Japan Participation Group, Los Alamos National Laboratory, the Max-Planck Institute for Astronomy (MPIA), New Mexico State University, University of Pittsburgh, University of Portsmouth, Princeton University, the United States Naval Observatory and the University of Washington (http://www.sdss.org). (http://www.sdss.org/). *2MASS* (*Two Micron All Sky Survey*) is a joint project of the University of Massachusetts and the Infrared Processing and Analysis Center/California Institute of Technology, funded by the National Aeronautics and Space Administration and the National Science Foundation. Hyperleda is an information system for astronomy based on the richest catalogue of homogeneous parameters of galaxies for the largest available sample (http://leda.univ-lyon1.fr). *NED (NASA/IPAC Extragalactic Database)* is operated by the Jet Propulsion Laboratory, California Institute of Technology, under contract with the National Aeronautics and Space Administration. *GALEX* (*Galaxy Evolution Explorer*) is a NASA Small Explorer, launched in April 2003 and developed in cooperation with the Centre National d'Études Spatiales of France and the Korean Ministry of Science and Technology. R is a free software environment for statistical computing and graphics (http://www.r-project.org/). TOPCAT is an interactive graphical tool for analysis and manipulation of tabular data (Taylor 2005) (http://www.star.bris.ac.uk/~mbt/topcat/).

References

Abazajian, K. N., Adelman-McCarthy, J. K., Agüeros, M. A., et al. 2009, ApJS, 182, 543
Allam, S. S., Tucker, D. L., Lin, H., & Hashimoto, Y. 1999, ApJ, 522, L89
Alongi, M., Bertelli, G., Bressan, A., et al. 1993, A&A, 97, 851
Alonso, S., Mesa, V., Padilla, N., & Lambas, D. G. 2012, A&A, 539, A46
Asari, N. V., Cid Fernandes, R., Stasińska, G., et al. 2007, MNRAS, 381, 263
Baldwin, J. A., Phillips, M. M., & Terlevich, R. 1981, PASP, 93, 5
Balogh, M. L., Morris, S. L., Yee, H. K. C., et al. 1999, ApJ, 527, 54
Bernardi, M., Nichol, R. C., Sheth, R. K., et al. 2006, AJ, 131, 1288
Bitsakis, T., Charmandaris, V., Le Floc'h, E., et al. 2010, A&A, 517, A75
Bitsakis, T., Charmandaris, V., da Cunha, E., et al. 2011, A&A, 533, A142
Borthakur, S., Yun, M. S., & Verdes-Montenegro, L. 2010, ApJ, 710, 385
Bressan, A., Fagotto, F., Bertelli, G., & Chiosi, C. 1993, A&A, 100, 647
Bruzual, G., & Charlot, S. 2003, MNRAS, 344, 1000
Byrd, G., & Valtonen, M. 1990, ApJ, 350, 89
Caon, N., Capaccioli, M., D'Onofrio, M., & Longo, G. 1994, A&A, 286, 39
Cardelli, J. A., Clayton, G. C., & Mathis, J. S. 1989, ApJ, 345, 245
Chabrier, G. 2003, PASP, 115, 763
Cid Fernandes, R., Sodré, L., Schmitt, H. R., & Leão, J. R. S. 2001, MNRAS, 325, 60
Cid Fernandes, R., Mateus, A., Sodré, L., Stasińska, G., & Gomes, J. M. 2005, MNRAS, 358, 363
Clemens, M. S., Bressan, A., Nikolic, B., & Rampazzo, R. 2009, MNRAS, 392, 35
Cole, S., Aragon-Salamanca, A., Frenk, C. S., Navarro, J. F., & Zepf, S. E. 1994, MNRAS, 271, 781
Cooper, M. C., Gallazzi, A., Newman, J. A., & Yan, R. 2010, MNRAS, 402, 1942
Coziol, R., & Plauchu-Frayn, I. 2007, AJ, 133, 2630
Coziol, R., Ribeiro, A. L. B., de Carvalho, R. R., & Capelato, H. V. 1998, ApJ, 493, 563
Coziol, R., Iovino, A., & de Carvalho, R. R. 2000, AJ, 120, 47
Coziol, R., Brinks, E., & Bravo-Alfaro, H. 2004, AJ, 128, 68
Coziol, R., Andernach, H., Caretta, C. A., Alamo-Martínez, K. A., & Tago, E. 2009, AJ, 137, 4795
Coziol, R., Torres-Papaqui, J. P., Plauchu-Frayn, I., et al. 2011, Rev. Mex. Astron. Astrofis., 47, 361
de la Rosa, I. G., de Carvalho, R. R., Vazdekis, A., & Barbuy, B. 2007, AJ, 133, 330
de Mello, D. F., Torres-Flores, S., & Mendes de Oliveira, C. 2008, ApJ, 135, 319
Deng, X.-F., He, J.-Z., & Wu, P. 2008, A&A, 484, 355
Dressler, A. 1980, ApJS, 42, 565
Durbala, A., del Olmo, A., Yun, M. S., et al. 2008, AJ, 135, 130
Fagotto, F., Bressan, A., Bertelli, G., & Chiosi, C. 1994, A&AS, 104, 365
Fujita, Y. 1998, ApJ, 509, 587
Gobat, R., Rosati, P., Strazzullo, V., et al. 2008, A&A, 488, 853
Henriksen, M., & Byrd, G. 1996, ApJ, 459, 82
Herberich, E., Sikorski, J., & Hothorn, T. 2010, PLoS, 5, 3
Hickson, P. 1982, ApJ, 255, 382
Hickson, P. 1997, ARA&A, 35, 357
Hickson, P., Kindl, E., & Huchra, J. P. 1988, ApJ, 331, 64
Hickson, P., Mendes de Oliveira, C., Huchra, J. P., & Palumbo, G. G. 1992, ApJ, 399, 353
Hothorn, T., Bretz, F., & Westfall, P. 2008, Biom J., 50, 346
Hoyle, B., Jimenez, R., & Verde, L. 2011, MNRAS, 415, 2818
Iglesias-Páramo, J., & Vílchez, J. M. 1997, ApJ, 479, 1901
Iglesias-Páramo, J., & Vílchez, J. M. 1998, ApJ, 518, 94
Iglesias-Páramo, J., & Vílchez, J. M. 1999, ApJ, 518, 94
James, P. A., Prescott, M., & Baldry, I. K. 2008, A&A, 484, 703
Jarrett, T. H., Chester, T., Cutri, R., et al. 2000, AJ, 119, 2498
Johnson, K. E., Hibbard, J. E., Gallagher, S. C., et al. 2007, AJ, 134, 1522
Karachentseva, V. E. 1973, Soobshch. Spets. Astroz. Obs., 8, 3
Kauffmann, G., White, S. D. M., & Guiderdoni, B. 1993, MNRAS, 264, 201
Kauffmann, G., Heckman, T. M., Tremonti, C., et al. 2003, MNRAS, 346, 1055
Kewley, L. J., Dopita, M. A., Sutherland, R. S., Heisler, C. A., & Trevena, J. 2001, ApJ, 556, 121
Kochanek, C. S., Pahre, M. A., Falco, E. E., et al. 2001, ApJ, 560, 566
Martin, D. C., Fanson, J., Schiminovich, D., et al. 2005, ApJ, 619, L1
Martínez, M. A., del Olmo, A., Coziol, R., & Focardi, P. 2008, ApJ, 678, 9
Martínez, M. A., Del Olmo, A., Coziol, R., & Perea, J. 2010, AJ, 139, 1199
Mateus, A., Sodré, L., Cid Fernandes, R., et al. 2006, MNRAS, 370, 721
Mendes de Oliveira, C., & Hickson, P. 1994, ApJ, 427, 684
Mendes de Oliveira, C., Coelho, P., González, J. J., & Barbuy, B. 2005, AJ, 130, 55
Menon, T. K. 1995, AJ, 110, 2605
Merritt, D. 1983, ApJ, 264, 24
Merritt, D. 1984, ApJ, 276, 26
Moles, M., del Olmo, A., Perea, J., et al. 1994, A&A, 285, 404
Nishiura, S., Shimada, M., Ohyama, Y., Murayama, T., & Taniguchi, Y. 2000, AJ, 120, 1691
Palumbo, G. G. C., Saracco, P., Hickson, P., & Mendes de Oliveira, C. 1995, AJ, 109, 1476
Paturel, G., Bottinelli, L., & Gouguenheim, L. 1994, A&A, 286, 768
Paturel, G., Andernach, H., Bottinelli, L., et al. 1997, A&AS, 124, 109
Pildis, R. A., Bregman, J. N., & Evrard, A. E. 1995, ApJ, 443, 514
Plauchu-Frayn, I., & Coziol, R. 2010a, AJ, 139, 2643
Plauchu-Frayn, I., & Coziol, R. 2010b, AJ, 140, 612
Proctor, R. N., Forbes, D. A., Hau, G. K. T., et al. 2004, MNRAS, 349, 1381
Ribeiro, A. L. B., de Carvalho, R. R., Coziol, R., Capelato, H. V., & Zepf, S. E. 1996, ApJ, 463, 5
Rubin, V. C., Hunter, D. A., & Ford, Jr., W. K. 1991, ApJS, 76, 153
Sánchez-Blázquez, P., Peletier, R. F., Jiménez-Vicente, J., et al. 2006, MNRAS, 371, 703
Schawinski, K., Kaviraj, S., Khochfar, S., et al. 2007, ApJS, 173, 512
Schlegel, D. J., Finkbeiner, D. P., & Davis, M. 1998, ApJ, 500, 525
Skrutskie, M. F., Cutri, R. M., Stiening, R., et al. 2006, AJ, 131, 1163
Sulentic, J. W. 1987, ApJ, 322, 605
Sulentic, J. W., Verdes-Montenegro, L., Bergond, G., et al. 2006, A&A, 449, 937
Taylor, M. B. 2005, ASPC, 347, 29
Thomas, D., Maraston, C., Bender, R., & Mendes de Oliveira, C. 2005, ApJ, 621, 673
Thomas, D., Maraston, C., Schawinski, K., Sarzi, M., & Silk, J. 2010, MNRAS, 404, 1775
Torres-Flores, S., Mendes de Oliveira, C., Amram, P., et al. 2010, A&A, 521, A59
Torres-Papaqui, J. P., Coziol, R., Ortega-Minakata, R. A., & Neri-Larios, D. M. 2012, ApJ, 754, 144
Tzanavaris, P., Hornschemeier, A. E., Gallagher, S. C., et al. 2010, ApJ, 716, 556
Verdes-Montenegro, L., Yun, M. S., Perea, J., del Olmo, A., & Ho, P. T. P. 1998, ApJ, 497, 89
Verdes-Montenegro, L., Yun, M. S., Williams, B. A., et al. 2001, A&A, 377, 812
Verdes-Montenegro, L., Del Olmo, A., Iglesias-Páramo, J., et al. 2002a, A&A, 396, 815
Verdes-Montenegro, L., Del Olmo, A., Yun, M. S., & Perea, J. 2002b, A&A, 430, 443
Verley, S., Leon, S., Verdes-Montenegro, L., et al. 2007, A&A, 472, 121
Vílchez, J. M., & Iglesias-Páramo, J. 1998, ApJS, 117, 1
Walker, L. M., Johnson, K. E., Gallagher, S. C., et al. 2010, AJ, 140, 1254
White, S. D. M., & Frenk, C. S. 1991, ApJ, 379, 52
Whitmore, B. C., Gilmore, D. M., & Jones, C. 1993, ApJ, 407, 489
Williams, B. A., & Rood, H. J. 1987, ApJS, 63, 265
Yi, S. K., Yoon, S.-J., Kaviraj, S., et al. 2005, ApJ, 619, L111
Zepf, S. E., Whitmore, B. C., & Levison, H. F. 1991, ApJ, 383, 524